RSC Advances

Arsenic removal from aqueous solution by adsorption using novel MiL-53(Fe) as highly efficient adsorbent

Journal:	*RSC Advances*
Manuscript ID:	RA-ART-10-2014-012326.R1
Article Type:	Paper
Date Submitted by the Author:	19-Nov-2014

Complete List of Authors:	Vu, Tuan; Institute of Chemistry - VAST, Surface Chemistry Le, Giang; Institute of Chemistry - VAST, Surface Chemistry Dao, Canh; Institute of Chemistry - VAST, Surface Chemistry Dang, Lan; TT Hue College of Education, Nguyen, Kien; Institute of Chemistry - VAST, Surface Chemistry Nguyen, Quang; Institute of Chemistry - VAST, Surface Chemistry Dang, Phuong; Institute of Chemistry - VAST, Surface Chemistry Tran, Hoa; Institute of Chemistry - VAST, Surface Chemistry Duong, Quang; Hue University of Education, Van Nguyen, Tuyen; Vietnam Academy of Science and Technology, Lee, Gun; Pukyung National University,

Arsenic removal from aqueous solution by adsorption using novel MiL-53(Fe) as highly efficient adsorbent

Tuan.A.Vu[1*], Giang.H.Le[1], Canh.D.Dao[1], Lan.Q.Dang[2], Kien.T.Nguyen[1], Quang.K.Nguyen[1], Phuong.T.Dang[1], Hoa.T.K.Tran[1], Quang.T.Duong[3], Tuyen.V.Nguyen[1] and Gun.D.Lee[4]

[1]Institute of Chemistry, Vietnam Academy of Science and Technology (VAST), 18 Hoang Quoc Viet, Cau Giay District, Hanoi, Vietnam
[2]College of education-Hue university, Vietnam, [3]Hue University of Education, Vietnam
[4]College of Engineering, Pukyong National University, 113, Engineering Building 4, Yongdang Campus, Busan, South Korea
Corresponding author: vuanhtuan.vast@gmail.com

Abstract

MiL-53(Fe) analogue was successfully synthesized by the HF free-solvothermal method. The sample was characterized by XRD, N_2 adsorption (BET), TEM, FTIR, XPS and AAS. From N_2 adsorption–desorption isotherms, it shows that the structure of MiL-53(Fe) in anhydrous form exhibits closed pores with almost no accessible porosity to nitrogen gas. XPS result reveals that Fe is really incorporated into MiL-53(Fe) framework. In hydrated form, pores of MIL-53(Fe) are filled with water molecules. Thus, MIL-53(Fe) exhibited very high adsorption capacity of As (V) in aqueous solution (Q_{max} of 21.27mg/g). From adsorption kinetics data, it reveals that As (V) adsorption isotherms fit the Langmuir model and obey the pseudo-second-order kinetic equation.

Keywords: novel MiL-53(Fe) adsorbent, arsenic removal, arsenic adsorption kinetics.

1 – Introduction

Metal-Organic Frameworks (MOFs) are a new class of hybrid materials assembled with metal cation and organic linker, have received a great attention in recent years due to their unique properties: high surface area, crystalline open structures, tunable pore size, functionality and their application in separation, gas storage, adsorption and catalysis [1, 8a-8d]. Some of the most interesting properties of MOFs are inherently linked with the secondary building units (SBUs) coordination sphere. Because of their site isolation, some SBUs feature metal cations with up to four open coordination site, priming them for inner-sphere redox reactivity [9]. Thus, metal substitution can alter directly the SBUs, creating the new properties of the material by introducing various metal centres in the same framework, one may cumulate different catalytically active sites and/or tune

adsorptive, optoelectronic, magnetic properties [10-14]. Recently, iron oxide as a promising adsorbent for removal of arsenic from aqueous solution has been investigated intensively [15–19] because the interaction between arsenic and iron oxide (micro and nano particles) is very strong and irreversible [19, 20]. In comparison to nanoparticles, metal−organic coordination polymers have the most important advantage is that the coordination polymers are tailored nanoporous host materials on the basis of the self-assembly of metal ions linked together by bridging ligands, which make the most striking difference from common materials and nanomaterials being probably the total lack of nonaccessible bulk volume in coordination polymer structures. One of the exceptional properties of MOFs relies on their ability to adapt their pore opening to accommodate guest species, and different modes of flexibility have been described [21,22]. This "breathing" effect and swelling can produce a dramatic increase or decrease in cell volume without a loss of crystallinity or bond breaking [23]. Typical examples are the porous chromium and aluminum terephthalates denoted MIL-53 (Cr) and MIL-53 (Al) [24,25]. The iron(III) analogue was also described [26], but in contrast with the Cr and Al based solids, which exhibit a permanent microporosity in the anhydrous state, its anhydrous form of MIL-53(Fe) exhibits closed pores with no accessible porosity to most gases [27-29]. The application of MiL-53 (Fe) is a litte reported. Very recently, Lunhong Ai et al [30] revealed that MIL-53(Fe) showed high photo-Fenton catalytic activity in organic dye degradation under visible light irradiation. In addition, it was claimed that Fe containing MOFs can be used as high effcient adsorbent for asenic removal. However, only a few papers on this topic were reported. Zhu et al [31] showed that Fe-BTC exhibited high asenic adsorption capacity (Q_{max} of 12,87mg/g), more than 6 times that of iron oxide nanoparticles with a size of 50 nm and 36 times that of commercial iron oxide powders.

In the present work, we report the synthsesis, characterization and asenic adsorption kinetic of MIL-53 (Fe). To our best knowledge, this is the first work reporting very high asenic adsorption capacity of MIL-53 (Fe) with Q_{max} of 21.27 mg/g.

2- Experimental section

Synthesis of MIL-53 (Fe)

MIL-53(Fe) was synthesized from a mixture of 10 mmol of terephthalic acid (Aldrich 98%), 5 mmol of iron (III) chloride hexahydrated (Aldrich, 99%) in 50 ml of N,N′-dimethylformamide (DMF, Aldrich, 98%). This slurry is then introduced in a 125 ml teflon lined autoclave. The system is then heated over night at 150^{o}C for 16h. The yellow

powder corresponding to the MIL-53 solid filled with DMF (MIL-53(DMF)) was obtained by filtration. To remove the occluded DMF, the solid was heated at 150°C on air overnight and then cooled down to room temperature. Further, to extract the residual traces of DMF, the solid was stirred during a few hours in a large volume of deionized water and finally filtered and dried at 60^{o}C over night.

Characterization

The powder X-ray diffraction (XRD) patterns of the samples were recorded on a Shimadzu XRD-6100 analyzer with Cu K_{α} radiation (l=1.5417Å). High resolution transmission electron microscopy (HR-TEM) using JEOL 1010 instrument operating at 80 kV with magnification of 25,000–100,000 was used to obtain HR-TEM photograps of the samples. The X-ray photoelectron spectroscopy (XPS) measurement was performed on the ESCALab MKII spectrometer using Mg K_{α} radiation. The FT-IR spectra of the samples were measured by the KBr pellet method (BIO-RAD FTS-3000). Surface Area of samples were determined on Quantachrome Instruments version 3.0 at 77K and using nitrogen adsorbate. Atomic absorption measurements for arsenic species were caried out using a Double-Beam Atomic Absorption Spectrophotometer AA-630 (Shimadzu corporation, Kyoto, Japan), equiped with a quartz T-tube cell and hydride vapor generation system HVG-1.

Removal efficiency of As(V) is defined as the following:

$$\text{Removal efficiency}\ (\%) = \frac{\text{initial conc. of As(V)} - \text{finnal conc. of As(V)}}{\text{initial conc. of As(V)}} x100$$

3 - Results and Discussion

3.1 characterization of the MiL-53(Fe)

X-ray Diffraction (XRD)

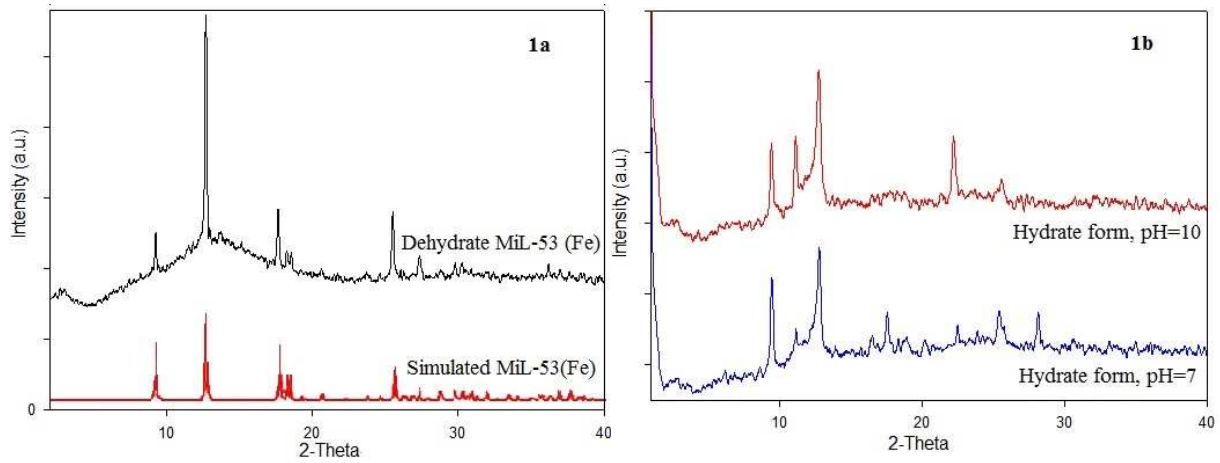

Fig.1 XRD patterns of MIL-53(Fe)

The XRD pattern of MIL-53(Fe) is plotted in Fig.1. In the pattern of the sample, the main diffraction peaks appear at 2θ of 9.24, 12.7, 17.66, 18.24, 18.58, 25.52, 27.32, 29.8, 30.28, 36.18 are identical to those reported for the MIL-53(Fe) phase [24-26]. The pattern of MIL-53(Fe) showed the flat background and high intensities, indicating high crystallinity of the samples. Additionly, no Fe_2O_3 or other phases were detected, indicating high purity of the sample. The influence of hydration – dehydration as well as pH value on MIL-53(Fe) phase were investigated. XRD paterns of hydrated-dehydrated MiL-53(Fe) at different pH values were showed in figure 1a and 1b. As observed in figure 1, the MiL-53(Fe) phase unpon hydration still remained the structure but the peak intensities were lower. For influence of pH on structure, at pH of 6-7, the MiL-53(Fe) phase is not changed but at higher pH value of 8 -10, the MiL-53(Fe) phase mainly remained but an intermediate phase appeared (fig.1b).

For MiL-53 materials, the behavior of hydrated – dehydrated phase is different. MiL-53(Cr) showed a hydrated phase with contracted pores and a dehydrated phase with open pores. In contrast, the loss of water from MIL-53(Fe) results in a closing of the structure to form the metastable anhydrous phase[27a]. Thus, Alhamami et al. [27b] review breathing behaviors of MOFs and show that in the case of MiL-53(Fe), the unit cell volume increased from 899.6 Å3 (dehydrated form) to 1973.5 $Å^3$ (hydrated form) and the channed diameter increased from 6.759 to 7.518 Å. The increase of unit cell volume is due to the increase of the distances between two nearest iron cations unpon hydration.

Transmission Electron Microscopy (TEM)

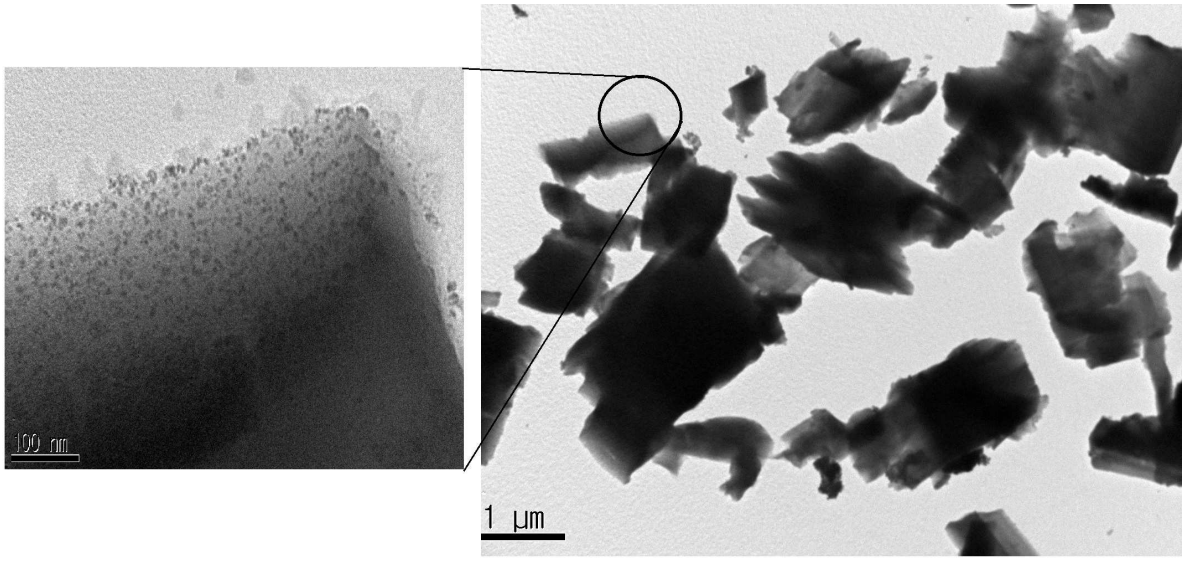

Fig.2. TEM photographs of MIL-53(Fe)

The morphology and particle size of the MIL-53(Fe) sample were examined by high resolution transmission electron microscopy (HR-TEM). The TEM image of MiL-53(Fe) and high magnification TEM image are illustrated in figure 2. As obserbed in Fig 2, the size distribution of MIL-53(Fe) crystals is not uniform and crystals size ranged from 1µm to 3 µm. The magnified TEM image reveales that very small pseudo-spherical particles of 5-8 nm, which closely attached on the surface of MiL-53 crystals.

N_2 adsorption–desorption isotherms

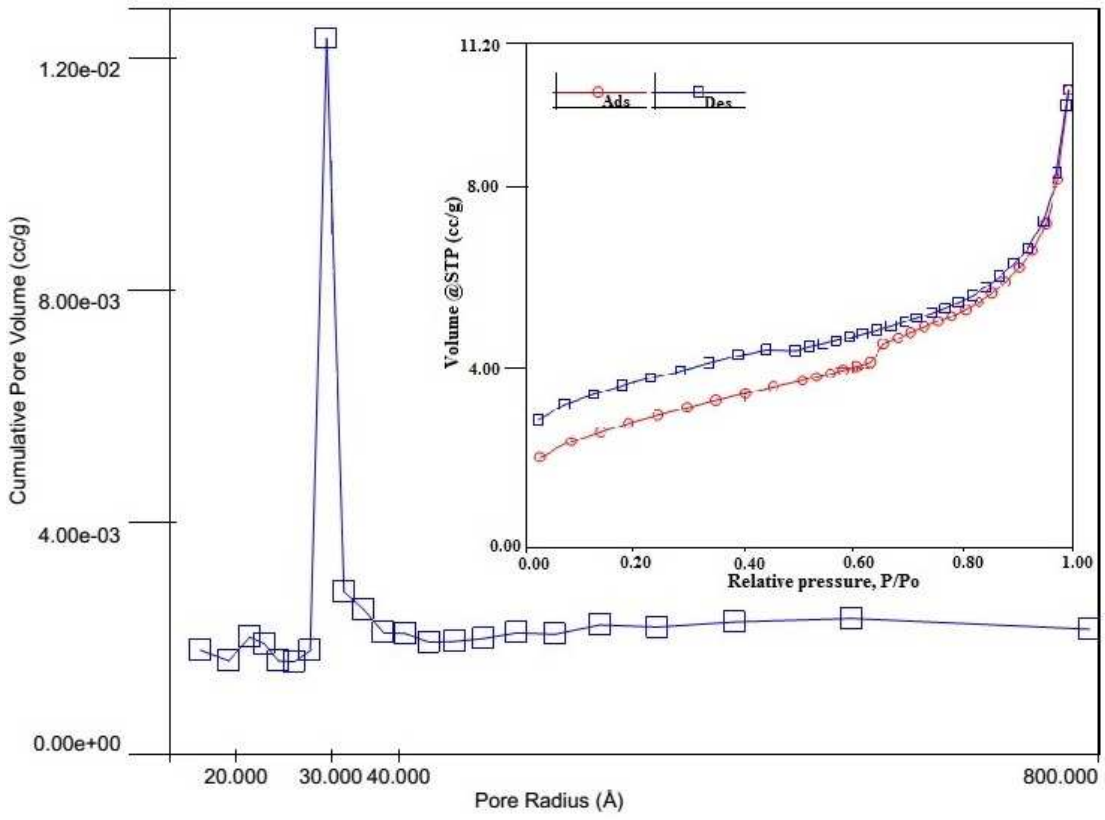

Figure 3. N_2 adsorption–desorption isotherms of MIL-53(Fe)

Specific surface area and pore volume of MiL-53(Fe) determined by N_2 adsorption-desorption isotherms at 77K. As seen in Fig 3, the N_2 adsorption-desorption curves displayed an intermediate mode between type I and IV, corresponding to the micropores and mesopores (Peng et al.2012). The Brunauer–Emmett–Teller (BET) surface area and total pore volume of MIL-53(Fe) were calculated to be 14 m^2/g and 0.012 cm^3/g, respectively. The Barrett–Joyner–Halenda (BJH) mesopore size distribution curve exhibited a pore size centered at about 2.9 nm (Fig. 3). The very low surface area observed on MIL-53(Fe) indicates that the anhydrous form of MIL-53(Fe) exhibits closed pores with almost no accessible porosity to nitrogen gas.

Fourier Transform Infrared Spectroscopy (FTIR)

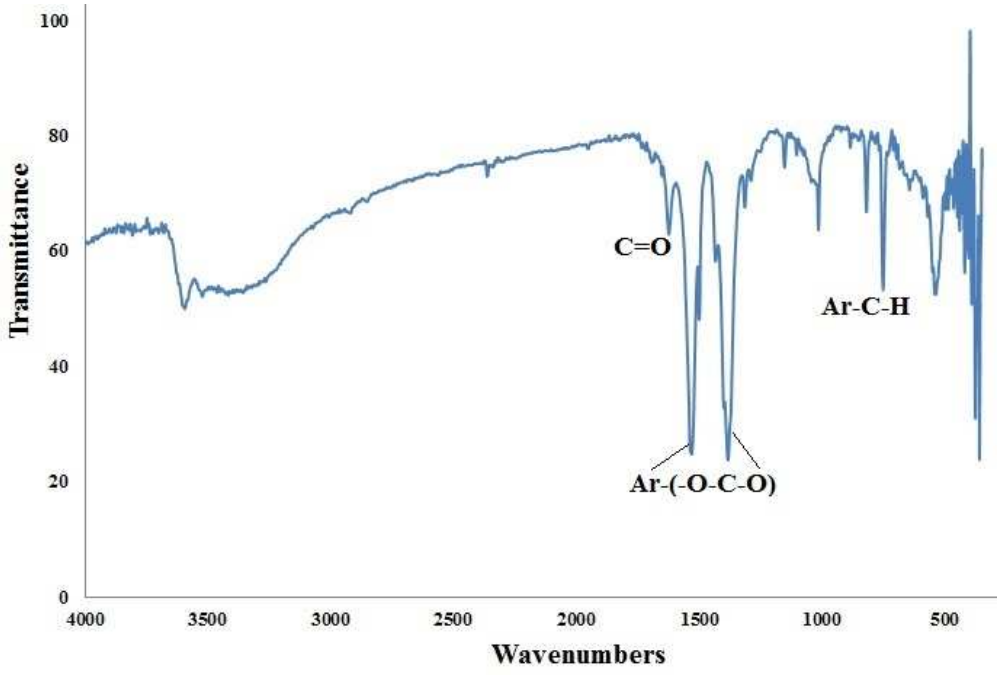

Fig.4. FTIR spectrum of MIL-53(Fe)

To identify the functional groups of MIL-53(Fe) sample, the FTIR spectroscopy was performed and the result is shown in Fig 4. The characteristic absorption peaks of the MIL-53(Fe) sample presented at 1680, 1543, 1396, 1020, and 750 cm^{-1}, which could mainly originate from the carboxylate groups vibrations and are identical to those of reported data in the literatures [33–35]. The broad peak centered at 3440 cm^{-1} is associated with the stretching vibrations of the O–H from the surface adsorbed water. The two sharp peaks at 1543 and 1396 cm^{-1} are assigned to asymmetric (ν_{as}(C–O)) and symmetric (ν_{as}(C–O)) vibrations of carboxyl groups, respectively, confirming the presence of the dicarboxylate linker within the sample. The peak at 750 cm^{-1} corresponds to C–H bending vibrations of the benzene. The intense peak at 540cm^{-1} is related to the Fe-O vibration [36].

X-ray photoelectron spectroscopy (XPS)

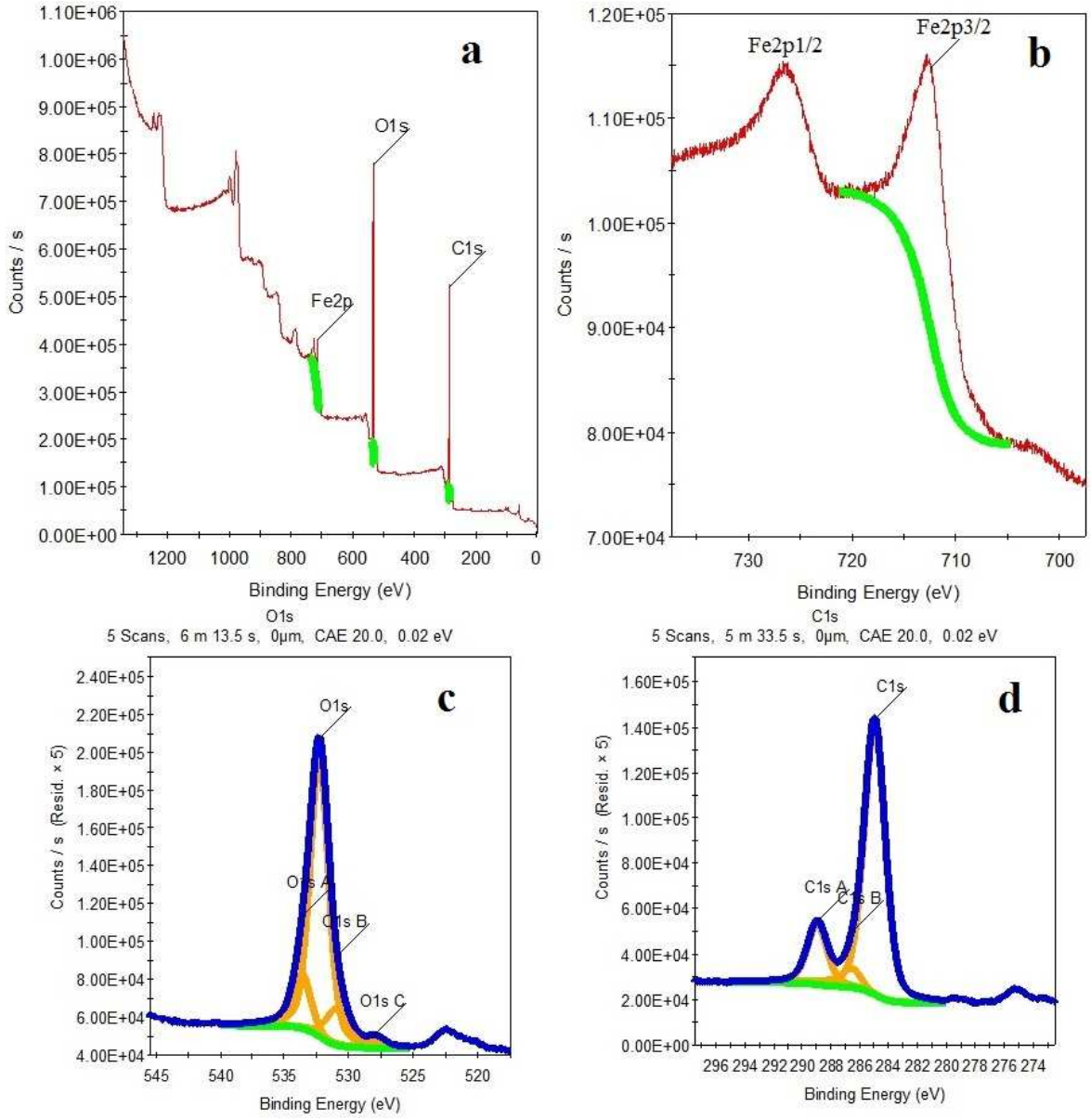

Fig. 5. XPS spectra of MIL-53(Fe)

XPS spectra of MIL-53(Fe) are shown in Fig.5. The XPS spectrum of C1s (Fig.5d) showed two peaks at 284.9 and 288.7 eV, corresponding to phenyl and carboxyl signals, respectively [31,37,38]. In the XPS spectrum of O1s (Fig.5c), the O1s peak at 531.7 and 533.1 eV related to the Fe-O-C species [39]. In the Fe 2p spectrum of MIL-53(Fe) (Fig.5b) appeared two peaks at 711.9 and 725.7 eV which correspond to Fe2p3/2 and Fe 2p1/2 signals [31,40]. From the XPS result, it can be concluded that Fe is really incorporated into MIL-53 framework.

3.2. Arsenic adsorption isotherms and kinetics

Arsenic adsorption isotherms

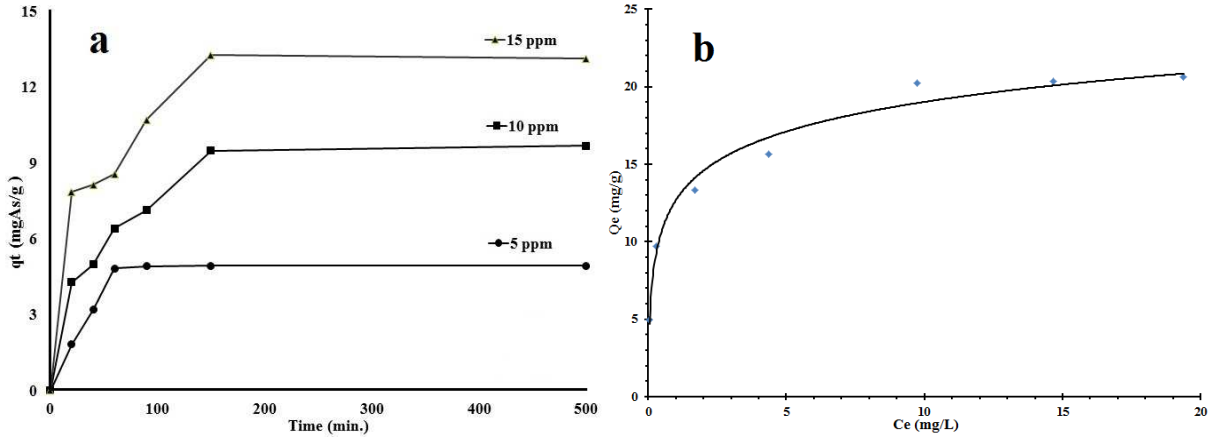

Fig. 6 (a) adsorption isotherms of MIL-53(Fe) at different initial As(V) concentrations and (b) relationship between adsorption capacity and concentrations at the equilibrium (pH = 5, Mass adsorbents/solution volume = 1.0 g/L, T = 298 K)

In order to investigate the ability of MIL-53(Fe) for As(V) removal, arsenic adsorption isotherms and kinetics were performed.

Figure 6 displays the dependence of As(V) adsorption capacity on adsorption time by MiL-53(Fe) at different initial As(V) concentrations of 5, 10 and 15 mg/L. The adsorption rates increased rapidly within first 60 minutes for all concentrations, indicating the attribution to the abundant free adsorptive sites and high As(V) concentrations gradient. Further increasing adsorption time, adsorption rates decreased. At different initial As(V) concentrations, necessary time to reach the equilibrium is distinguished, i.e. at initial As(V) concentration of 5mg/L is only 90 minutes while at higher concentrations of 10-15 mg/L, longer time (120 mins) is needed (Fig 6a). The relationship between adsorption capacity at the equilibrium (Qe) and concentrations at the equilibrium (Ce) is presented in Fig 6b. As observed in Fig 6b, with increasing concentrations at the equilibrium (low concentrations of 0-10 mg/L), adsorption capacity at the equilibrium lineal increased. However, at higher concentrations of 10-20 mg/L, adsorption capacity negligible increased, already reaching the saturation state.

Effect of pH

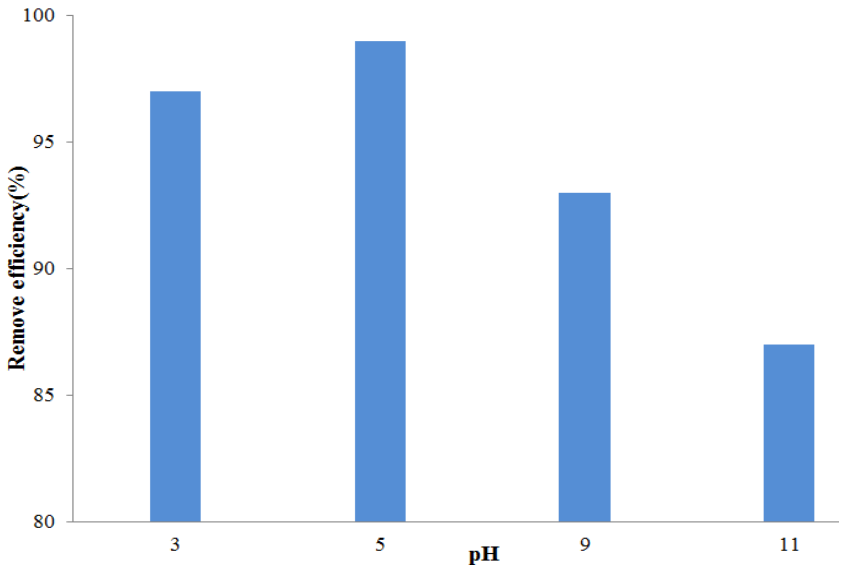

Fig 7. Effect of pH on removal efficiency of As(V) over MiL-53(Fe)
(initial As(V) concentration: 5 mg/L, m /V = 1.0 g/L, T = 298 K)

The pH is one of most important factors on arsenic adsorption process. $H_2AsO_4^-$ dominates at low pH, which is less than about pH 6.9 [41]. To optimine pH values for adsorption of As(V) on MiL-53(Fe), the uptake of As(V) as a function of pH was investigated. Removal efficiency of As(V) in the range of pH 3−11 is illustrated in figure 7. As seen in Fig 7, the maximum of As(V) removal efficiency on MiL-53(Fe) was about 99% at pH of 5. Further increasing to pH of 11, the removal efficiency of As(V) decreased to 87%. It was argued that generally, MOFs materials are unstable in strong base condition (especially in the case used terephtalic acid as linker herein) and dissolved gradually, consequently the removal efficiency of As(V) decreased. High As(V) adsorption capacity of MiL-53(Fe) can be explained by the fact that at pH <6.9, As(V) in aqueous solution dominated $H_2AsO_4^-$, an anionic ligand with an ability to donate a pair of electrons (lewis base) which strongly interacts with centered Fe^{3+} cations(Lewis acid) in MiL-53(Fe) framwork by Lewis acid-base interaction. Additionally, electrostatic interaction between centered Fe^{3+} cations in MiL-53 framwork and anionic $H_2AsO_4^-$ in aqueous solution occurs. The combination of these two interactions leads to enhance the As(V) adsorption capacity of MiL-53(Fe), consequently.

Adsorption Isotherms

Table 1. Langmuir and Freundlich isotherm constants for As (V) at room temperature

Langmuir and Freundlich isotherm constants			
Langmuir *isotherm*		Freundlich *isotherm*	
Q_o ($mg.g^{-1}$)	21,27	1/n	0.264
K_L ($L.mg^{-1}$)	2,13	K_F $[(mgg^{-1})(mg^{-1})^{1/n}]$	11,57
R^2	0.994	R^2	0.972
R_L	0.08	-	-

Two empirical equations, Langmuir and Freundlich isotherms models, were often used to analyze the experimental data [42,43].

The Langmuir equation is expressed as follows:

$$\frac{C_e}{q_e} = \frac{1}{q_m K_L} + \left(\frac{1}{q_m}\right) C_e$$

The Freundlich equation is expressed as follows

$$\log q_e = \log K_F + \left(\frac{1}{n}\right) \log C_e$$

Where q_m and K_L in the Langmuir equation represent the maximum adsorption capacity of adsorbents (mg/g) and the Langmuir constant related to the energy of adsorption, respectively. K_F and n are Freundlich constants related to adsorption capacity and adsorption intensity, respectively. The parameters of the Langmuir and Freundlich models were calculated and given in table 1. The curves fitting results of the Langmuir and Freundlich model are shown in Figure 8.

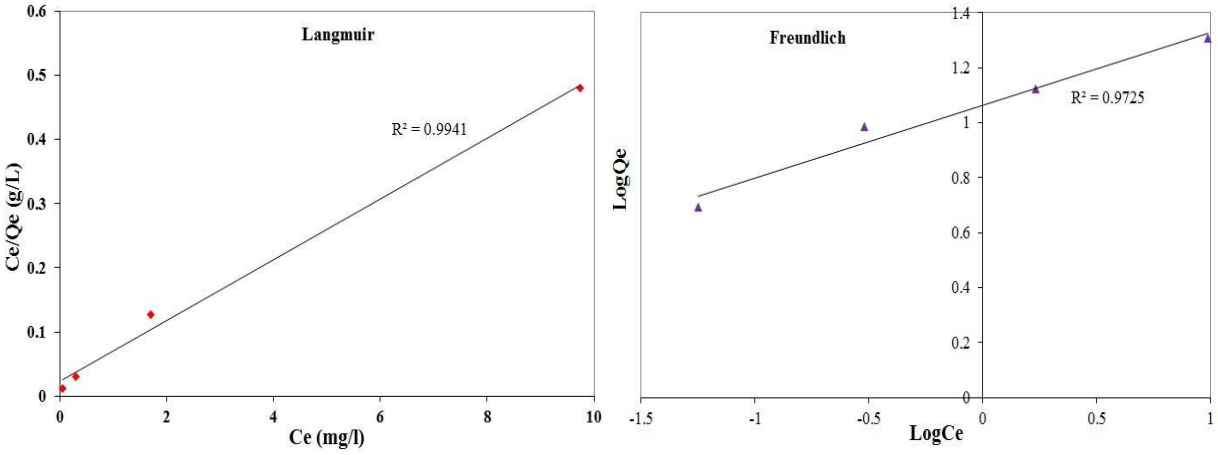

Figure 8. (a) linearized Langmuir and (b) linearized Freundlich isotherms for As(V) adsorption on MiL-53(Fe)

As observed in table 1 and Fig. 8, the value of R^2= 0,994 for Langmuir model is higher than that of R^2=0,972 for Freundlich model, indicating that the Langmuir model fits much better than the Freundlich model.

It is well accepted that the Langmuir isotherm assumes a surface with homogeneous binding sites, whereas the Freundlich isotherm is based on an exponential distribution of adsorption sites and adsorption onto heterogeneous surfaces.

As seen in the magnified HR-TEM image (Fig. 2), the Fe-oxo clusters with the size of 5-8 nm which uniform distributed on the MiL-53(Fe) surface, indicating the homogeneous adsorption sites of the sample. Therefore, this result further supports the confirmation that the Langmuir model fits much better than the Freundlich model. Moreover, much higher adsorption capacity (Q_{max} of 21.27 mg/g) of MiL-53(Fe) as compared to that of the Fe_2O_3 containing adsorbents or Fe containing MOFs reported in the literature (see table 2) was noted.

Table 2: Comparison of As (V) adsorption capacity for different adsorbents

No	Adsorbents	Experimental conditions	Q_{max} (mg/g)	Ref.
1	Granular ferric hydroxide	pH=6.5, T=293 K, I=0.02 mol/L NaCl	3.1	44
2	PAC 20-modified montmorillonite	pH=6.9, T=298 K, m/V=2.0 g/L	3.6	45
3	Iron-containing granular activated carbon	pH=4.7, T=298 K, m/V=3.0 g/L	6.6	46
4	Fe^{3+} oxide coated ethylenediamine	pH=4.0, T=298 K,	10.4	47

	functionalized MWCNT	m/V=0.1 g/L		
5	Iron and 1,3,5-Benzenetricarboxylic Metal−Organic Coordination Polymers	pH = 4,m /V = 5.0 g/L, T = 298 K	12.87	31
6	Mil 53(Fe)	pH = 5 ,m /V = 1.0 g/L, T = 298 K	21.27	This study

Adsorption kinetics

Pseudo- first order equation

The rate constant of adsorption is determined from the pseudo-first order equation given by Langergren and Svenska [48]:

$$\ln(q_e - q_t) = \ln q_e - k_1 t$$

Where q_e and q_t are the amounts of As (V) adsorbed ($mg.g^{-1}$) at equilibrium and at time t (min), respectively, and k_1 the rate adsorption constant ($min.^{-1}$). Figure 9 presents plots of $\ln(q_e\text{-}q_t)$ versus time t for different As(V) concentrations. Values of k_1 were calculated from the plots of $\ln(q_e - q_t)$ versus t for different concentrations of As (V) on Mil-53(Fe) and given in table 3. As observed in table 3, the low value of R^2 as well as large difference in q_e experimental and q_e calculated values indicate that the As (V) adsorption on Mil-53(Fe) does not obey the pseudo-first order equation.

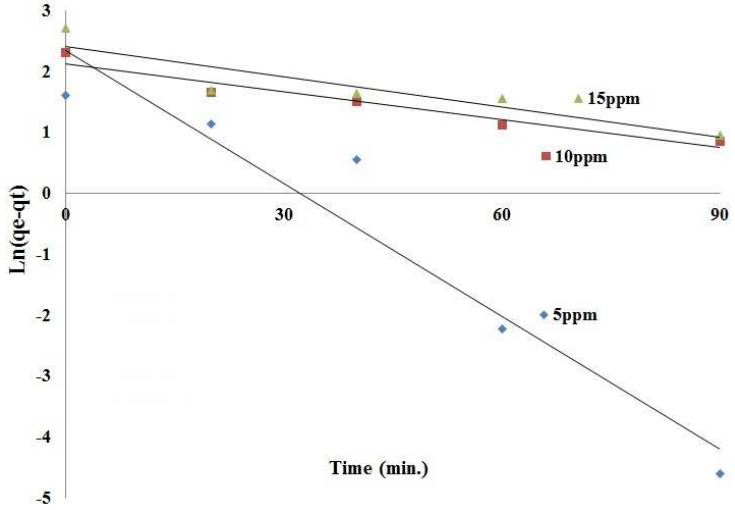

Figure 9. Plots of $\ln(q_e\text{-}q_t)$ versus time t for different As(V) concentrations

Table 3: Rate adsorption constants and As(V) adsorption capacities calculated according to pseudo-first order equation

Conc. (*mg/l)*	Equations	R_1^2	k_1 (min^{-1})	$q_{e,\,exp}$ (mg/g)	$q_{e,\,cal}$ (mg/g)
5	$\ln(q_e-q_t) = 2{,}404-0{,}016.t$	0,833	0,016	4.94	11,06
10	$\ln(q_e-q_t) = 2{,}129-0{,}015.t$	0,934	0,015	9.7	8,404
15	$\ln(q_e-q_t) = 2{,}346-0{,}072.t$	0,926	0,072	13.301	10,44

Pseudo- second order equation

On the other hand, a pseudo-second order equation based on equilibrium adsorption [49] is expressed as:

$$\frac{t}{q_t} = \frac{1}{k_2 q_e^2} + \frac{1}{q_t} t$$

Where k_2 (g/mg.min) is the rates constant of pseudo-second order adsorption. If pseudo-second order kinetics is applicable, the plot of t/q versus t should show a linear relationship. There is no need to know any parameter beforehand and qe and k_2 can be determined from the slope and intercept of the plot. Also, this procedure is more likely to predict the behavior over the whole range of adsorption. The linear plots of t/q versus t are presented in figure 10.

correlation coefficients, q_e experimental and q_e calculated values according to the pseudo-second order kinetic equation are shown in table 4. As noted in tab.4, the high R^2 values of 0.994-0.996 as well as the coincidence between q_e experimental and q_e calculated values, it can confirm that the As(V) adsorption in aqueous solution obeys the pseudo-second order kinetic equation.

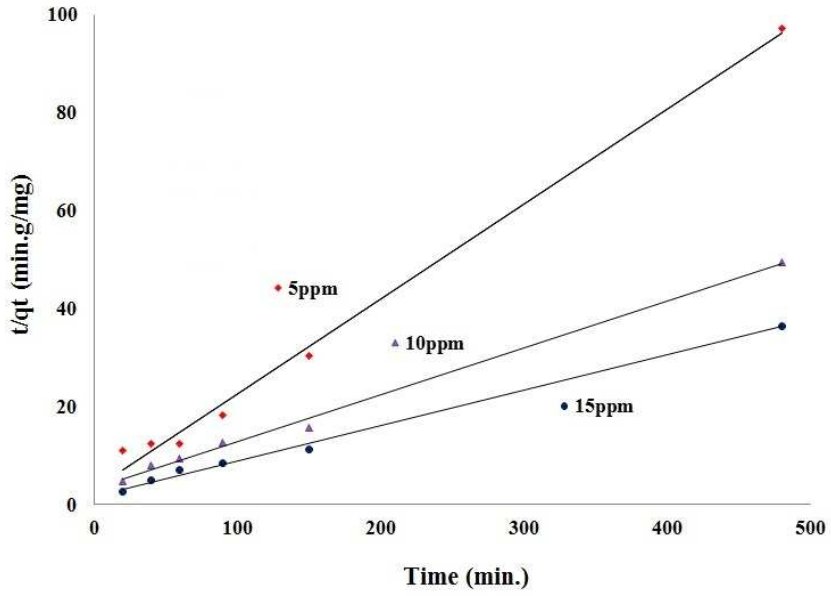

Figure 10 . Linear plots of t/q versus time t for different As(V) concentrations

Table 4: Rate adsorption constants and As(V) adsorption capacities calculated according to pseudo-second order equation

Conc. (*mg/l*)	Equations	R_2^2	k_2(*g/mg.min*)	$q_{e,\ exp}$ (*mg/g*)	$q_{e,\ cal}$ (*mg/g*)
5	$\frac{t}{q_t} = 3{,}135+0.193t$	0.994	0,0120	4.94	5.18
10	$\frac{t}{q_t} = 3{,}253+0.095.t$	0.996	0,0032	9.7	10,5
15	$\frac{t}{q_t} = 1{,}673+0{,}072.t$	0.996	0,0031	13.301	13.88

Conclusion

From the obtained results, some conclusions can be drawn:

- MIL-53(Fe) analogue with high purity and crystallinity was successfully synthesized by the HF free-solvothermal method.
- From N_2 adsorption–desorption isotherms, it shows that the structure of MiL-53(Fe) in anhydrous form exhibits closed pores with almost no accessible porosity

to nitrogen gas. XPS result reveals that Fe is really incorporated into MIL-53(Fe) framework.

- In hydrated form, pores of MIL-53(Fe) are filled with water molecules. Thus, MIL-53(Fe) exhibited very high adsorption capacity of As (V) in aqueous solution (21.27mg/g).
- From adsorption kinetics data, it reveals that As (V) adsorption isotherms fit the Langmuir model and obey the pseudo-second order kinetic equation.

Acknowledgments

The authors thanks the National Foundation for Science and Technology Development of Vietnam—NAFOSTED **(Grant no. 104.05-2013.64)** for financial support.

References

[1]. O. V. Zalomaeva, K. A. Kovalenko, Y. A. Chesalov, M. S. Mel'gunov, V. I. Zaikovskii, V. V. Kaichev, A. B. Sorokin, O. A. Kholdeeva and V. P. Fedin, Dalton Trans., (2011) 40, 1441–1444.

[2]. C. K. Brozek and M. Dincă, J. Am. Chem. Soc., (2013) 135, 12886–12891.

[3]. N. A. Khan and S. H. Jhung, J. Hazard. Mater, (2013) 260 (15), 1050–1056.

[4]. T. R. Cook, Y.R. Zheng and P. J. Stang, Chem. Rev., (2013) 113 (1), 734–777.

[5]. S. T. Meek, J. A. Greathouse and M. D. Allendorf, Adv. Mater, (2011) 23, 249–267.

[6]. H. Wu, Q. Gong, D. H. Olson and J. Li, Chem. Rev., (2012) 112, 836–868.

[7]. J.-R. Li, J. Sculley and H.-C. Zhou, Chem. Rev., (2012) 112, 869–932.

[8]. (a). P. Horcajada, R. Gref, T. Baati, P. K. Allan, G. Maurin, P. Couvreur, G. F´erey, R. E. Morris and C. Serre, Chem. Rev, (2012) 112, 1232–1268. (b). Zhangjing Zhang, Zi-Zhu Yao, Shengchang Xiang and Banglin Chen, Energy Environ. Sci., 2014,7, 2868-2899. (c). Shengchang Xiang, Yabing He, Zhangjing Zhang, Hui Wu, Wei Zhou, Rajamani Krishna, Banglin Chen, Nature Commun.,

2012, 3, 954. (d). Shengchang Xiang, Wei Zhou, Zhangjing Zhang, Mark A. Green, Yun Liu and Banglin Chen, Angew. Chem. Inter. Ed. 2010, 49, 4615-4618.

[9]. M. Dincă, A. Dailly, Y. Liu, C. M. Brown, D. A. Neumann and J. R. Long, J. Am. Chem. Soc., (2006) 128 (51), 16876–16883.

[10]. A. Dhakshinamoorthy, M. Alvaro and H. Garcia, Chem. Commun., (2012) 48, 11275–11288.

[11]. A. Phan, A. U. Czaja, F. G´andara, C. B. Knobler and O. M. Yaghi, Inorg. Chem., (2011) 50 (16), 7388–7390.

[12]. E. D. Bloch, L. J. Murray, W. L. Queen, S. Chavan, S. N. Maximoff, J. P. Bigi, R. Krishna, V. K. Peterson, F. Grandjean, G. J. Long, B. Smit, S. Bordiga, C. M. Brown and J. R. Long, J. Am. Chem. Soc., (2011) 133 (37), 14814–14822.

[13]. Y. Fu, D. Sun, Y. Chen, R. Huang, Z. Ding, X. Fu and Z. Li, Angew. Chem., Int. Ed., (2012) 51, 3364–3367.

[14]. C. K. Brozek and M. Dincă, Chem. Sci., (2012) 3, 2110–2113.

[15]. Pan, YF.; Chiou, CT.; Lin, TF. Environ Sci Pollut Res Int. (2013) 20 (3):1899.

[16]. Gu, B. H.; Schmitt, J.; Chen, Z. H.; Liang, L. Y.; Mccarthy, J. F, Environ. Sci. Technol., (1994) 28 (1), 38–46.

[17]. Zhang, Y.; Yang, M.; Huang, X, Chemosphere, (2003) 51, 945-952.

[18]. Guo X J, Chen F H, Environ. Sci. Technol, (2005) 39, 6808-18.

[19]. Iesan C.M, Capat C, Ruta F, Udrea I, Water Res, (2008) 42, 4327-33.

[20]. Kanel S.R, Manning B, Charlet L, Choi H, Environ. Sci. Technol., (2005) 39 (5), 1291–1298.

[21]. Li D, Kaneko K, Chem. Phys. Lett. (2001) 335, 50–56.

[22]. Kitaura R, Seki K, Akiyama G, Kitagawa S, Angew. Chem., Int. Ed. (2003) 42, 428–431.

[23]. Serre C, Mellot-Draznieks C, Surble S, Audebrand N, Filinchuk Y, Fe´rey G, Science 30 March (2007), Vol. 315 no. 5820, 1828-1831.

[24]. Serre C, Millange F, Thouvenot C, Nogue`s M, Marsolier G, Loue¨r D, Fe´rey G, J. Am. Chem. Soc.(2002) 124, 13519–13526.

[25]. Loiseau T, Serre C, Huguenard C, Fink G, Taulelle F, Henry M, Bataille T, Fe´rey G, Chem. Eur. J. (2004), Vol 10, No 6, 1373–1382.

[26]. Tabatha R. Whitfield, X Wang, Lumei Liu, Allan J. Jacobson , Solid State Sciences (2005) 7, 1096–1103.

[27]. (a) Millange F, Guillou N, Walton R. I, Greneche J.M, Margiolaki I Férey G , Chem. Commun.(2008) 4732–4734. (b) Mays Alhamami, Huu Doan and Chil-Hung Cheng, A Review on Breathing Behaviors of Metal-Organic-Frameworks (MOFs) for Gas Adsorption, Materials 2014, 7, 3198-3250

[28]. Devautour-Vinot S, Maurin G, Henn F, Serre C, Devic T, Férey G, Chem. Comm.(2009) 19, 2733–2735.

[29]. Volkringer C, Loiseau T, Guillou N, Férey G, Elkaïm E, A Vimont, Dalton Trans. (2009) 2241–2249.

[30]. Lunhong Ai, Caihong Zhang, Lili Li, Jing Jiang, Applied Catalysis B: Environmental (2014) 148–149, 191–200.

[31]. Bang-Jing Zhu, Xin-Yao Yu, Yong Jia, Fu-Min Peng, Bai Sun, Mei-Yun Zhang, Tao Luo, Jin-Huai Liu and Xing-Jiu Huang, J. Phys. Chem. C, (2012) 116, 8601−8607.

[32]. L. Peng, J. Zhang, J. Li, B. Han, Z. Xue, G. Yang, Chem. Commun. (2012) 48, 8688–8690

[33]. P. Horcajada, C. Serre, G. Maurin, N.A. Ramsahye, F. Balas, M. Vallet-Regí, M. Sebban, F. Taulelle, G. Férey, J. Am. Chem. Soc. (2008) 130, 6774–6780.

[34]. T. Devic, P. Horcajada, C. Serre, F. Salles, G. Maurin, B. Moulin, D. Heurtaux, G. Clet, A. Vimont, J.-M. Grenèche, B. Le Ouay, F. Moreau, E. Magnier, Y. Filinchuk, J. Marrot, J.-C. Lavalley, M. Daturi, G. Férey, J. Am. Chem. Soc. (2010) 132, 1127–1136.

[35]. A. Banerjee, R. Gokhale, S. Bhatnagar, J. Jog, M. Bhardwaj, B. Lefez, B. Hannoyer, S. Ogale, J. Mater. Chem. (2012) 22, 19694–19699

[36]. R. Fazaeli, H. Aliyanb, M. Moghadam and M. Masoudinia, J. Mol. Catal. A: Chem., (2013) Vol 374–375, 46–52.

[37]. J. A. Gardella, S. A. Ferguson and R. L. Chin, Appl. Spectrosc., (1986),40 (2), 224–232.

[38]. L. J. Gerenser, J. Vac. Sci. Technol., A, (1990), 8, 3682.

[39]. S. Srivastava, S. Badrinarayanan and A. Mukhedkar, Polyhedron, (1985), 4, 409-414.

[40]. T. Yamashita and P. Hayes, Appl. Surf. Sci., (2008), 254, 2441–2449

[41]. Mohan D, Pittman Jr C, J. Hazard. Mater. Vol 142, No 1–2, (2007), 1–53.

[42]. Li Y. H, Liu F. Q, Xia B, Du Q. J, Zhang P, Wang D. C, Wang Z. H, Xia Y. Z, J. Hazard. Mater. (2010), 177 (1-3), 876-880.

[43]. Zhao X. W, Jia Q, Song N. Z, Zhou W. H, Li Y. S, J. Chem. Eng. Data (2010), 55, 4428-4433.

[44]. Banerjee K, Amy G. L, Prevost M, Nour S, Jekel M, Gallagher P. M, Water Res. (2008), 42, 3371-3378

[45]. Zhao S, Feng C, Huang X, Li B, Niu J, Shen Z, J. Hazard. Mater. (2012) Vol 203–204, 317–325.

[46]. Gu Z, Fang J, Deng B, Environ. Sci. Technol. (2005) 39, 3833-3843.

[47]. Velivckovic Z, Vukovic G. D, Marinkovic A. D, Moldovan M. S, Peric-Grujic A. A, Uskokovic P. S, Ristic M. D, Chem. Eng. J. (2012) 181, 174-181.

[48]. Langergren S, Kungliga Svenska Vetenskapsakademiens. Handlingar, (1898) 24 (4) : 1-39.

[49]. Y.S. Ho, G. McKay, Chem. Eng. J. (1998) 70, 115–124.

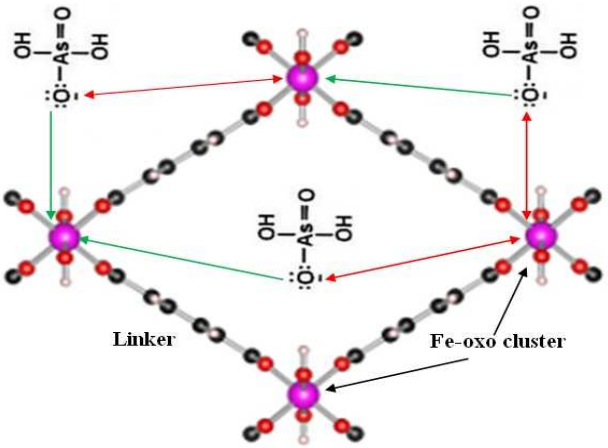

GA As(V) adsorption based on Lewis acid-based and electrostatic interactions over MiL-53 (Fe)